



Estimation of gas record alteration in very low accumulation ice cores

Kévin Fourteau¹, Patricia Martinerie¹, Xavier Faïn¹, Alexey A. Ekaykin², Jérôme Chappellaz¹, and Vladimir Lipenkov²

¹Univ. Grenoble Alpes, CNRS, IRD, Grenoble INP, IGE, F-38000 Grenoble, France

²Climate and Environmental Research Laboratory, Arctic and Antarctic Research Institute, St. Petersburg, 199397, Russia

Correspondence: kevin.fourteau@univ-grenoble-alpes.fr or patricia.martinerie@univ-grenoble-alpes.fr

Abstract. We measured the methane mixing ratios of enclosed air in five ice core sections drilled on the East Antarctic plateau. Our work aims to study two effects that affect the recorded gas concentrations in ice cores: layered gas trapping artifacts and firn smoothing. Layered gas trapping artifacts are due to the heterogeneous nature of polar firn, where some strata might close early and trap abnormally old gases that appear as spurious values during measurements. The smoothing is due to the combined effects of diffusive mixing in the firn and the progressive closure of bubbles at the bottom of the firn. Consequently, the gases trapped in a given ice layer span a distribution of ages. Concentration measurements thus only measure the average value in the ice layer, which removes the fast variability from the record. We focus on the study of East Antarctic plateau ice cores, as these low accumulation ice cores are particularly affected by both layering and smoothing. Our results suggest that the presence of layering artifacts in deep ice cores is linked with the chemical content of the ice. We use high-resolution methane data to parametrize a simple model reproducing the layered gas trapping artifacts for different accumulation conditions typical of the East Antarctic plateau. We also use the high-resolution methane measurements to estimate the gas age distributions of the enclosed air in the five newly measured ice core sections. It appears that for accumulations below $2\text{cm}\cdot\text{ie}\cdot\text{yr}^{-1}$ (ice equivalent) the gas records experience nearly the same degree of smoothing. We therefore propose to use a single gas age distribution to represent the firn smoothing observed in the glacial ice cores of the East Antarctic plateau. Finally, we used the layered gas trapping model and the estimation of glacial firn smoothing to estimate their potential impacts on a million-and-a-half years old ice core from the East Antarctic plateau. Our results indicate that layering artifacts are no longer individually resolved in the case of very thinned ice near the bedrock. They nonetheless contribute to slight biases of the measured signal (less than 10ppbv and 0.5ppmv in the case of methane and carbon dioxide). However, these biases are small compared to the dampening experienced by the record due to firn smoothing.



1 Introduction

The East Antarctic plateau is characterized by low temperatures and low accumulation rates. The low precipitations create the conditions for the presence of very old ice near the domes of the region (Raymond, 1983; Martín and Gudmundsson, 2012). Thanks to this particularity, the ice core retrieved at Dome C, within the EPICA project, has been dated back to 800,000
5 years in the past (Bazin et al., 2013; Veres et al., 2013). The analysis of the ice, and of the bubbles within, has made possible the reconstruction of the Earth past temperatures and atmospheric concentrations in major greenhouse gases over the last eight glacial cycles (Lüthi et al., 2008; Loulergue et al., 2008). In turn, this knowledge helps us to better understand the Earth climate system and its past and future evolutions (Shakun et al., 2012). Furthermore, there is currently an active search for ice older than one-and-a-half million years within the European Beyond EPICA-Oldest Ice project. Most of the potential drilling sites
10 for such old ice are located on the East Antarctic plateau (Fischer et al., 2013; Van Liefferinge and Pattyn, 2013; Passalacqua et al., 2018). Within the next decade, we might therefore expect the retrieval of new deep ice cores at low accumulation drilling sites of East Antarctica, with ages reaching back to one-and-a-half million years or more.

However, the gas records in low accumulation ice cores should not be directly interpreted as images of the atmospheric
15 history. Indeed, due to the very process of gas trapping in the ice, two distinct effects might create discrepancies between the actual atmosphere's history and its imprint in the ice. The first one is due to the heterogeneous structure of the firn when transforming into airtight ice. The overall structure of the firn column is characterized by a progressive increase in density with depth, associated with the constriction of the interstitial pore network (Stauffer et al., 1985; Arnaud et al., 2000; Salamatin et al., 2009). At high enough densities, pores in the firn pinch and isolate the interstitial air from the atmosphere (Stauffer
20 et al., 1985). However, firn is a highly stratified medium (Freitag et al., 2004; Fujita et al., 2009; Hörhold et al., 2012; Gregory et al., 2014) and some of the strata might experience early (respectively late) pore closure when compared to the rest of the firn (Etheridge et al., 1992; Martinerie et al., 1992). Consequently, abnormal strata might enclose older (respectively younger) air than their immediate surroundings, creating age irregularities in the gas record (Mitchell et al., 2015; Rhodes et al., 2016). In turn, the irregularities appear as spurious values in the measured gas record (Rhodes et al., 2016; Fourteau et al., 2017).
25 These anomalies have been referred to as layered gas trapping artifacts and do not reflect actual atmospheric variations. The second effect that creates differences between the atmosphere and its imprint in the ice, is due to the combination of diffusive air mixing in the firn (Schwander, 1989) and the progressive closure of pores in a firn stratum (Schwander et al., 1993; Mitchell et al., 2015). Consequently, the air enclosed in a given ice layer does not originate from a single point in time, but is rather characterized by a continuous age distribution covering tens to hundreds of years (Schwander et al., 1988; Schwander et al.,



1993; Rommelaere et al., 1997). Therefore, the concentration measured in an ice stratum is an average of atmospheric concentrations over a period of time. This effect removes the fast variability from the record, and has therefore been referred to as the smoothing effect (Spahni et al., 2003; Joos and Spahni, 2008; Köhler et al., 2011; Ahn et al., 2014; Fourteau et al., 2017). The degree of alteration between the atmosphere and its recording is strongly dependent on the local precipitation rate, with low accumulation ice cores being particularly affected both in terms of gas layered artifacts (Rhodes et al., 2016; Fourteau et al., 2017) and in terms of smoothing (Spahni et al., 2003; Joos and Spahni, 2008; Köhler et al., 2011; Ahn et al., 2014; Fourteau et al., 2017).

In order to properly evaluate the composition of past atmospheres based on the gas records in polar ice cores, it is thus necessary to characterize the specificities of those two effects. For the smoothing, the gas age distributions can be calculated, in the case of modern ice cores, using gas trapping models parameterized by firn pumping and pore closure data (Buizert et al., 2012; Witrant et al., 2012). However, to estimate the gas age distribution in bubbles it is necessary to use a closed porosity profile in firn. Such closed porosity profiles are associated with large uncertainties (Schaller et al., 2017). Moreover, a specific problem arises in the case of glacial ice cores from East Antarctica. They were formed under very low precipitation rates, below $2\text{cm}\cdot\text{ie}\cdot\text{yr}^{-1}$ (ice equivalent, Veres et al., 2013; Bazin et al., 2013), and temperatures that have no known equivalent nowadays. Thus, gas trapping models cannot be constrained and used to estimate the gas age distributions responsible for smoothing during glacial periods. Concerning layered gas trapping, it originates from firn heterogeneities and is therefore a stochastic process. Moreover, current gas trapping models do not fully represent the centimeter scale variability of the firn. The proper modelling of layered gas trapping is thus limited by the lack of knowledge of glacial firn heterogeneities and the difficulty to model gas trapping in a layered medium. Fourteau et al. (2017) proposed an empirical model to reproduce the artifacts observed in the Vostok ice core during the Dansgaard-Oeschger event 17. However, this model has only been applied to this particular event and might not be directly applicable for different periods and conditions.

For this work, we analyzed methane concentrations in five ice core sections from the East Antarctic plateau. These sections cover accumulation and temperature conditions representative of East Antarctica for both the glacial and inter-glacial periods. The new data are used to parameterize a revised version of the gas layered trapping model proposed by Fourteau et al. (2017). Our goal is to render this model applicable to a range of accumulation rates characteristic of glacial and inter-glacial conditions on the East Antarctic plateau. Then, the gas age distributions for each of the five records are estimated by comparing the low accumulation records with much higher accumulation records (Fourteau et al., 2017). Finally, we simulate gas trapping in a



hypothetical million-and-a-half years old and thinned ice core, including gas layering artifacts. We then simulate the process of methane measurements using a continuous flow analysis system, and of carbon dioxide measurements using a discrete method. The synthetic signals are finally compared to the original atmospheric reference to quantify the deterioration of atmospheric information.

5 2 Methods

2.1 Choice and description of the studied ice cores

The newly measured ice core sections originate from the East Antarctic sites of Vostok, Dome C, and Lock-In. The three sites are displayed on a map in Figure 1. The five measured sections correspond to time periods where high resolution methane measurements from high-accumulation ice cores are also available.

10

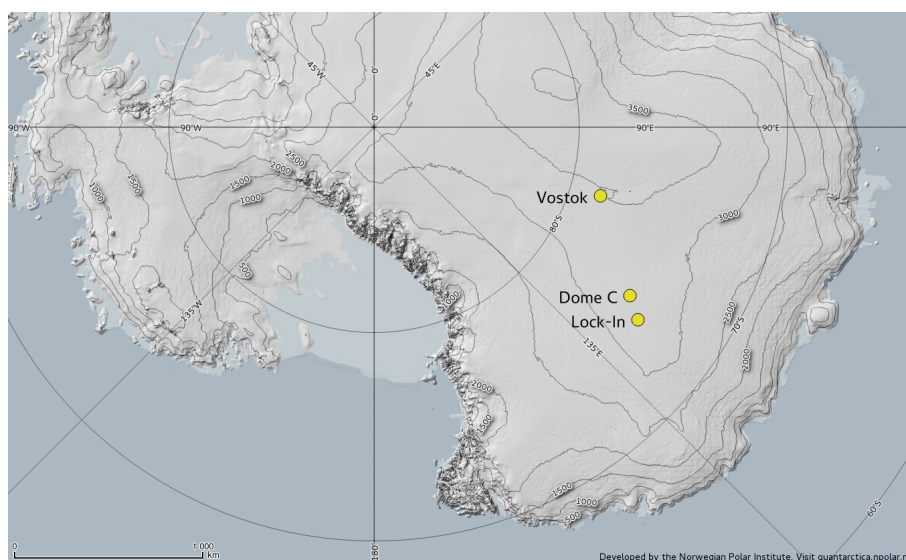


Figure 1. Map of the East Antarctic plateau with the sites of Lock-In, Dome C, and Vostok shown (made with the Quantartica package).

Modern Lock-In ice core:

The first studied ice core section is the upper part of the Lock-In ice core. The site of Lock-In is located 136km away from Dome C, towards the coast (3209m above sea level, coordinates 74°08.310' S, 126°09.510' E). The local accumulation is of 3.9cm.yr⁻¹ (Yeung et al., 2019). About 80m of ice was analyzed for methane, ranging from 116m (near the firn-ice transition) to 200m depth. The last firn air pumping during drilling operation was conducted at 108.3m depth. The gas record ranges

15



from 500 to 3000yrBP (Before Present, with present defined as 1950 in this article).

Modern Dome C ice core:

A shallow ice core from Dome C was analyzed for depths ranging from 108 to 178m. Similarly to Lock-In, this section corresponds to ages ranging from 500 to 3000yrBP, but is characterized by a lower accumulation rate of $2.7\text{cm}\cdot\text{ie}\cdot\text{yr}^{-1}$ (Gautier et al., 2016).

Holocene Dome C ice core:

Ice from the second drilling of the EPICA Dome C ice core (referred to as EDC99 hereafter) was measured from 312 to 338m depth. According to the AICC2012 chronology, the gas ages range from 7950 to 9000yrBP, with an average accumulation of $3.1\text{cm}\cdot\text{ie}\cdot\text{yr}^{-1}$ (Bazin et al., 2013; Veres et al., 2013). This period includes the 8.2ka cold event (Thomas et al., 2007), notably characterized by a sharp decrease in global methane concentrations (Spahni et al., 2003; Ahn et al., 2014).

DO6-9 Dome C ice core:

A section from the first drilling of the EPICA Dome C ice core (referred to as EDC96 hereafter) was analyzed for depths ranging from 690 to 780m. The AICC2012 chronology indicates gas ages covering the period 33000 to 41000yrBP, and an average accumulation rate of $1.5\text{cm}\cdot\text{ie}\cdot\text{yr}^{-1}$ (Bazin et al., 2013; Veres et al., 2013). The Dansgaard-Oeschger (DO) events 6 to 9 are included in this gas record (Huber et al., 2006; Chappellaz et al., 2013).

DO21 Vostok ice core:

The last analyzed section originates from the Vostok 4G ice core, for depths between 1249 and 1290m. The expected gas ages span from 84000 to 86500yrBP, with an average accumulation of $1.5\text{cm}\cdot\text{ie}\cdot\text{yr}^{-1}$ (Bazin et al., 2013; Veres et al., 2013). This section was chosen as it includes the record of the DO21 event, the fastest methane increase of the last glacial period (Chappellaz et al., 2013).

2.2 High-resolution methane measurements

The five ice core sections were analyzed for methane concentrations using a Continuous Flow Analysis (CFA) system, including a laser spectrometer based on optical-feedback cavity enhanced absorption spectroscopy (OF-CEAS; Morville et al., 2005), at the Institut des Géosciences de l'Environnement (IGE), Grenoble, France. The IGE's CFA apparatus and data processing



procedure are described in greater details in Fourteau et al. (2017). The five ice core sections were melted at an average rate of $3.6\text{cm}\cdot\text{ie}\cdot\text{yr}^{-1}$, which allows to access centimeter scale variations in the methane record. However, the measured concentrations are affected by the preferential dissolution of methane in the meltwater (Chappellaz et al., 2013; Rhodes et al., 2013). It is therefore necessary to apply a correction factor to account for this effect. However, this factor is a priori not known and potentially ice core dependent. The methodology for correcting for methane dissolution will be addressed in Section 3.1 below.

3 Results and Discussion

3.1 Correction for methane dissolution in the meltwater

In order to correct the measured mixing ratios for the preferential dissolution of methane in water, a correction factor is applied to the data to raise them to absolute values (Chappellaz et al., 2013; Rhodes et al., 2013). One way to estimate this correction factor is to compare the dissolution-affected CFA data with records that are already on an absolute scale.

The discrete methane measurements from the high accumulation WAIS Divide (WD) ice core published by Mitchell et al. (2013) cover the period from 500 to 3000yrBP. We therefore use the WD data to estimate the correction factors for the modern sections of Lock-In and Dome C.

Loulergue et al. (2008) performed discrete methane measurements in the Dome C EPICA ice core, that include the 8.2ka, DO6 to 9, and DO21 events. We use these discrete methane data to correct our CFA data for the dissolution, for the Holocene and DO6-9 Dome C ice core sections and for the DO21 event section in Vostok.

Note that in the case where our CFA data and the absolute scale measurements do not originate from the same ice core, the match between the datasets are performed on sections with low methane variability to reduce the influence of firn smoothing. The signals after correction for the dissolution of methane are displayed in light blue in the upper panels of the Figures 2 to 6. The gas age chronologies indicated in the figures will be constructed in Section 3.4.1 of this article. The black superimposed curves in Figures 4 to 6 correspond to the part of the signal cleaned for layering artifacts, as described in Section 3.3.3. The correction factors found are close to 1.13.

3.2 Atmospheric references

In Sections 3.3.2 and 3.4.1 below, weakly smoothed methane gas records will be used as atmospheric references to study gas trapping in low accumulation ice cores. As it is important that these gas records contain enough fast variability to be used as



atmospheric references, we use methane gas records from much higher-accumulation ice cores (Fourteau et al., 2017). For the modern Lock-In and Dome C sections, we use the discrete measurements from the WD ice core, also used for correcting the methane preferential dissolution (Mitchell et al., 2013). For the Holocene section of EDC99, we used CFA data from an ice core drilled at Fletcher promontory as the atmospheric reference (Robert Mulvaney and Xavier Faïn, personal communication),
5 completed with discrete data from Louergue et al. (2008) for the oldest part of the period (depths below 330m in Figure 4). For the DO6-9 events section in the EDC96 ice core, we use high-resolution CFA data from the WD ice core (Rhodes et al., 2015). The WD gas record dating has been made consistent with the AICC2012 and GICC chronologies following Buizert et al. (2015). Finally, the atmospheric reference used for the Vostok DO21 period is based on the NEEM CFA record published by Chappellaz et al. (2013). As the Vostok and NEEM sites are in different hemispheres, it is necessary to take into account the
10 inter-hemispheric methane gradient between the two sites. We evaluated this inter-hemispheric gradient to be 30ppbv for the DO21 period. This value is in line with the work of Dällenbach et al. (2000). Yet, it remains possible that the inter-hemispheric gradient is not constant during this period of global methane rise. The use of a high resolution and weakly smoothed Antarctic record as the atmospheric reference would resolve this inter-hemispheric gradient problem, but such a record is not available. Using a spline version of the data of Chappellaz et al. (2013), we observe that it is not possible to find a gas age distribution
15 able to reproduce the smoothing over the all section (Figure S1 of the Supplement). This suggests that the NEEM record cannot be directly used as an atmospheric reference for Vostok, due to the smoothing of the fast event at the onset of the DO21 (around the 1260m depth in Figure 6). To retrieve the full variation of this fast event, we used a "deconvolution" technique similar to the ones in Witrant and Martinerie (2013) and Yeung et al. (2019). The effect of the deconvolution is to increase the amplitude of the fast event at the onset of the DO21, which in turn increases the consistency between the NEEM and Vostok methane
20 records. Note that the deconvolution method requires gas age distributions for the NEEM ice core as input. The age distributions enclosed in NEEM vary over the DO21 event due to the large variation in accumulation at this site during the period. The gas age distributions in the NEEM ice core are estimated with gas trapping models forced with various accumulation conditions (Bock et al., 2012, personal communication Patricia Martinerie). The atmospheric references are displayed as orange dashed lines in the lower panels of Figure 2 to 6.

25 3.3 Layered trapping artifacts

It has been observed in the high-accumulation firn of DE08 that not all layers close at the same depth (Etheridge et al., 1992), and that the air in summer layers is generally older than in winter layers. Building on this idea, Mitchell et al. (2015) and Rhodes et al. (2016) proposed that the layering observed at the firn-ice transition induces gas stratigraphic irregularities and

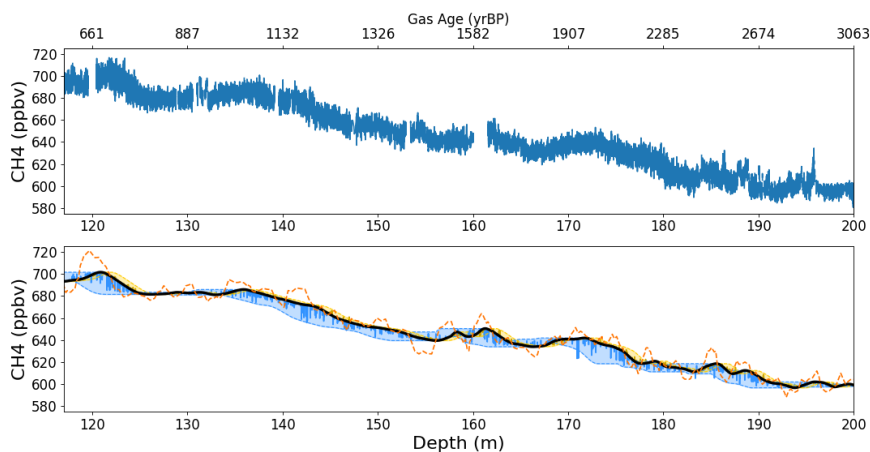


Figure 2. Measured and modeled modern Lock-In methane profile. Upper panel: High resolution methane measurements in light blue. Lower panel: Modeled layering artifacts. The black curve is the expected signal without artifacts. The blue and yellow spikes respectively are randomly distributed early and late closure artifacts. The blue and yellow shaded areas respectively correspond to the range of early and late artifacts with density anomalies up to two standard deviations. The dashed orange curve is the record used as the atmospheric reference.

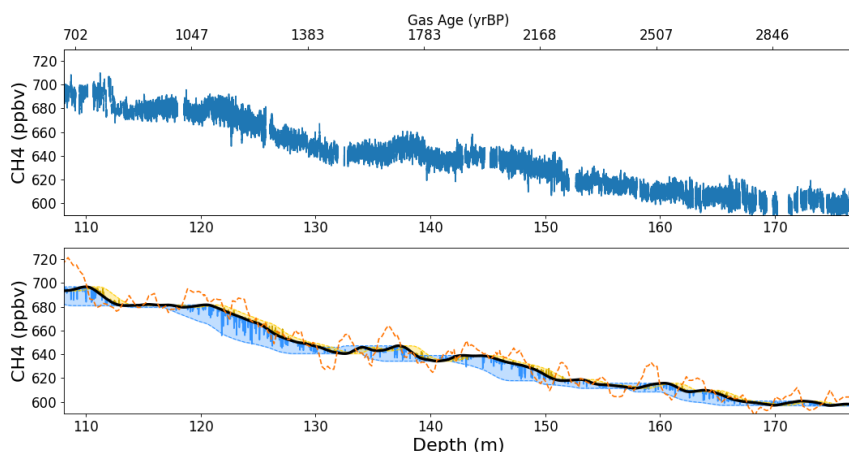


Figure 3. Same as Figure 2 for the modern Dome C section.

age inversions in the record. Rhodes et al. (2016) and Fourteau et al. (2017) used such stratigraphic heterogeneities to explain the observation of sudden variations in high resolution methane records. These abrupt methane variations do not correspond to actual atmospheric variations and have been called layered trapping artifacts, or more simply layering artifacts. The mechanism producing them is that layers closing especially early (or late) contain air older (or younger) than their immediate surroundings.

- 5 During periods of variations of atmospheric composition, the methane mixing ratios in these layers are thus different than in their surroundings and appear as anomalous values (Rhodes et al., 2016).

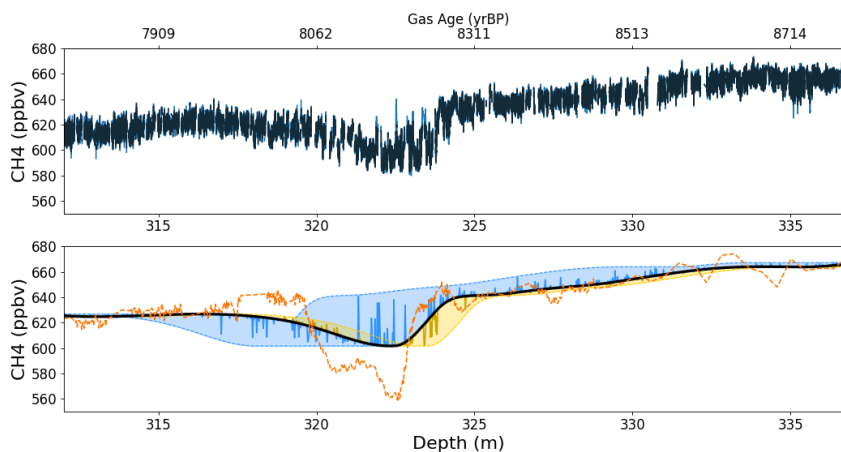


Figure 4. Same as Figure 2 for the Holocene EPICA Dome C section. In addition the superimposed black signal in the upper panel shows the data cleaned of layering artifacts

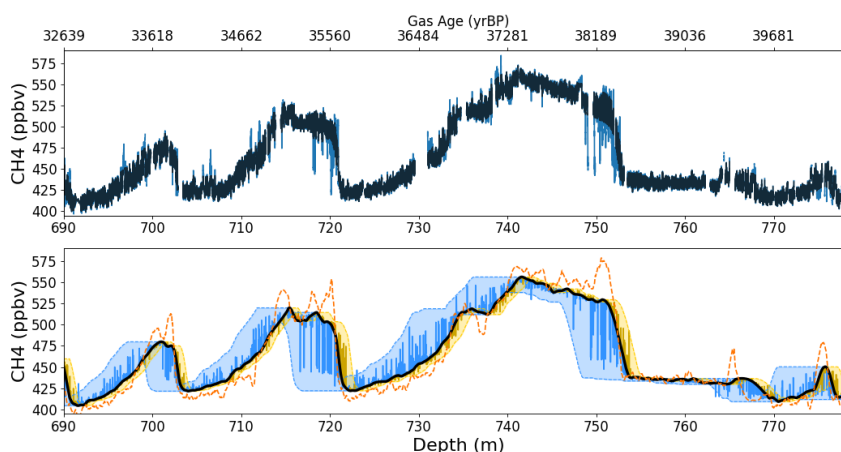


Figure 5. Same as Figure 4 for the DO6-9 EPICA Dome C section.

In accordance with Rhodes et al. (2016) and Fourteau et al. (2017), we observe abrupt variations in the methane records, larger than the analytical noise of ~ 10 ppbv, during periods of variations in atmospheric concentrations. These layering artifacts are notably well marked during the onset of DO events 8 and 21, corresponding to 750 and 1252m depth in the EDC96 and Vostok ice cores, respectively in Figure 5 and 6. A zoom of the EDC96 record is available in Figure S2 of the Supplement to display the layering artifact. They appear as reduced methane concentration layers near the onset of the DO events, and cannot therefore be explained by contamination issues. The layered trapping artifacts tend to disappear in the absence of marked atmospheric variations. This explains the absence of important layering artifacts in the Lock-In and Dome C modern records (Figures 2 and 3). Fourteau et al. (2017) pointed out that one of the data points of the DO8 event in the EPICA Dome C methane record

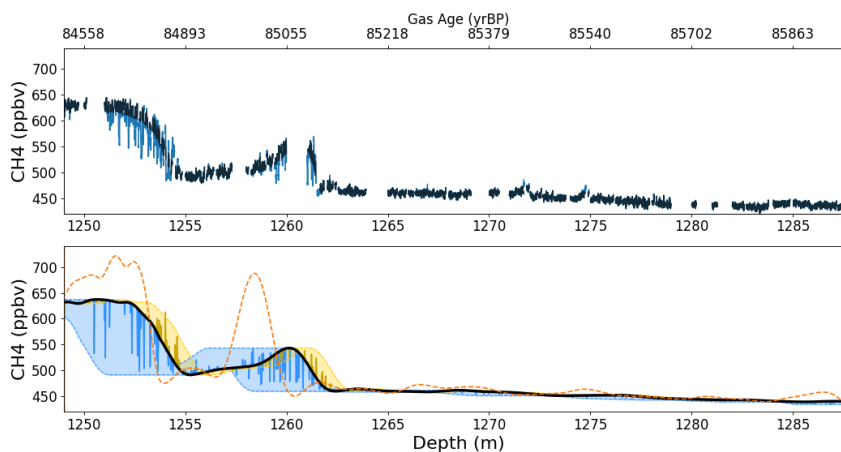


Figure 6. Same as Figure 4 for the DO21 Vostok section.

published by Louergue et al. (2008) might have been sampled in an early closure layer, and thus represents a spurious value in their record. By comparing our new high-resolution record with the one of Louergue et al. (2008), we confirm that this data point does not correspond to atmospheric variability, and that it was sampled in a zone with a high number of early closure artifacts (see Figure S3 of the Supplement).

- 5 Important late closure artifacts are unusual in methane gas records. The new measurements confirm this observation. Late closure artifacts, that should appear as positive methane anomalies at the onset of the DO events, are almost absent in our measurements. This can be explained by the fact that the surrounding firm layers are already sealed and prevent long distance gas transport, which in turn prevents the late closure layers to enclose young air (Fourteau et al., 2017).

3.3.1 Impact of chemistry on layered gas trapping

- 10 The EDC96 methane data suggest a lack of layering artifacts affecting the DO6 event (around the 700m depth in Figure 5). We counted only 14 layering artifacts that clearly stand out of the analytical noise on the 20m long section between 695 and 715m. For a comparison, we counted 15 artifacts on the 4m long section from 718 to 722m (DO7 event). These sections are not directly comparable as they did not undergo the same atmospheric methane variations during bubble enclosure, but it nonetheless suggests that the upper section of the DO6-9 record shows a lower number of layering artifacts per meter. Previous
15 studies have highlighted the role of chemical impurities for the presence of dense strata in polar firn. Hörhold et al. (2012) and Fujita et al. (2016) argue that the presence of ions can soften the firn and facilitate the densification of some strata.

To evaluate the potential impact of ions on layered gas trapping artifacts in the EDC96 methane record, we compared the high resolution methane data with total calcium data measured in the ice phase (Lambert et al., 2012). We chose to focus



on calcium since high resolution data are readily available and Hörhold et al. (2012) observed a correlation between calcium content and the density of firn layers. However, as pointed out by Hörhold et al. (2012) and Fujita et al. (2016), calcium should not be seen as the ion responsible for the preferential densification of firn, but rather as a proxy for the general ionic content. A comparison of the two datasets is shown in Figure 7. The depth difference between the EDC96 ice core, in which the methane measurements were performed, and the EDC99 ice core, in which the calcium measurements were performed, was taken into account using volcanic markers (Parrenin et al., 2012). The calcium data clearly show a transition between two parts: ice below the depth 718m is characterized by relatively high calcium values and a high variability, while ice above 718m is characterized by low calcium values and a low variability. The transition between these two parts corresponds to the high methane plateau of the DO7 event. It also matches with the transition described above between the two regions of large and small numbers of layering artifacts. It therefore appears that the number of significant artifacts (standing out of the analytical noise) is correlated to the variability of calcium concentrations. It is consistent with the mechanisms proposed in the literature: calcium variability is associated with a general ionic concentration variability that creates particularly dense strata in the firn (Hörhold et al., 2012; Freitag et al., 2013; Fujita et al., 2016). These strata then close in advance and trap young air that appears as layering artifacts (Rhodes et al., 2016; Fourteau et al., 2017).

We then evaluated the calcium levels for the other studied ice core sections. Using the data of Lambert et al. (2012), it appears that the 8.2ka and modern periods of Dome C are characterized by low calcium levels and variability. Similar low calcium levels and variability at Lock-In have been observed by chemistry measurements (data not presented here). Unfortunately, high resolution chemistry data are not available for Vostok. Assuming that the calcium variability is similar at Dome C and Vostok, the data from Lambert et al. (2012) indicate that the DO21 period displays low calcium level and variability, while the DO17 period studied by Fourteau et al. (2017) shows high calcium level and variability, similar to the DO7 to 9 period.

3.3.2 Modeling layered trapping artifacts

The ability to model layered gas trapping helps quantifying and predicting its impact on gas records. For this purpose, we revised the simple layered gas trapping model proposed by Fourteau et al. (2017) for the Vostok DO17 section. Our aim is to parametrize the model in order to reproduce the layering artifacts observed in the new five measured sections, as well as in the previously published DO17 section of the Vostok core. This layered trapping model is based on the physical assumption that the density anomaly of a layer (its density difference with the bulk behavior) can directly be converted into a trapping depth

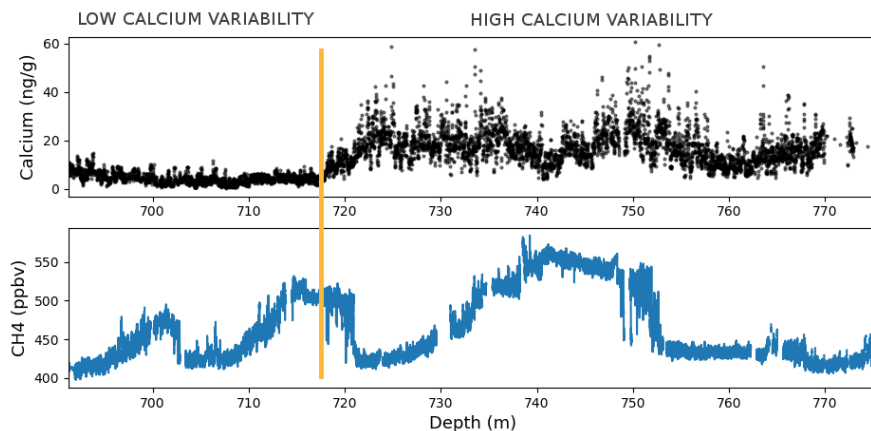


Figure 7. Upper panel: calcium concentrations measured in the EPICA Dome C ice core section covering the DOs 6 to 9 (Lambert et al., 2012). Lower panel: methane mixing ratios measured in this study.

anomaly (the difference in closing depth with the bulk behavior). The computation of depth anomalies is given by:

$$\Delta z = \frac{\Delta \rho}{\partial_z \rho} \quad (1)$$

where Δz is the depth anomaly of a given layer, $\Delta \rho$ its density anomaly, and $\partial_z \rho$ the derivative of the bulk firm density with depth in the trapping zone. For the rest of the article $\partial_z \rho$ will be referred to as the densification rate. The methane concentration in an early trapping layer is then simply the concentration trapped by the bulk firm at a depth Δz below. Fourteau et al. (2017) model is based on the computation of the age anomalies of abnormal layers (the time difference between the closure of the layers and the bulk behavior). However, this age-based formulation is sensitive to the dating of the ice core, and can lead to abnormally strong artifacts where the chronology is poorly constrained. On the other hand, the depth-based formulation proposed here (Equation 1) is not affected by dating uncertainties.

10

The model requires a densification rate for the firm-ice transition zone. Observations of density profiles in Dome C and Vostok proposed by Bréant et al. (2017) reveal densification rates around $2.2 \text{ kg} \cdot \text{m}^{-4}$ for both sites. This value also applies to the Lock-In firm as inferred from high resolution density measurements (Fourteau et al., 2019). Therefore, the densification rate was set at $2.2 \text{ kg} \cdot \text{m}^{-4}$ for all sites studied here. Finally, the model requires a typical density anomaly in the closing part of the firm. Based on the linear relationships of density standard deviation with temperature and accumulation proposed by Hörhold et al. (2011), Fourteau et al. (2017) estimated the typical density anomaly to be $5 \pm 2 \text{ kg} \cdot \text{m}^{-3}$ for the Vostok firm during the

15



glacial DO17 event. Moreover, Hörhold et al. (2011) report a density standard deviation of $4.6\text{kg}\cdot\text{m}^{-3}$ around the firn-ice transition of the Dome C site. As a first guess, we set the density anomalies Δ_ρ to obey a zero-centered Gaussian distribution of standard deviation $5\text{kg}\cdot\text{m}^{-3}$. Similarly to Fourteau et al. (2017), the depth anomalies of late closure layers are reduced by 75% in order to replicate their low impact in the measured records.

- 5 While this parametrization produces adequate results for most of the gas records studied here, it results in a clear underestimation of the layering artifacts for the DO events 7 and 8 in the EDC96 ice core (Figure S4 of the Supplement). Our understanding is that the layering model fails to take into account the impact of high calcium variability during this period. To introduce the influence of calcium in the model, we simply increase the typical density anomaly during period of high calcium variability, by applying an enhancing factor of 1.5. This enhancing factor was chosen to produce visually correct results in the case of the high calcium variability period of the DO7 to 9 (depths below 718m in the EDC96 record). For consistency, we also applied this enhancing factor for the DO17 period in Vostok, as this period displays a calcium variability similar to the DO 7 and 9 period.

The modeled artifacts are displayed below the newly measured signals in Figures 2 to 6, and the modeled artifacts for the DO17 in Vostok with the new calcium parametrization are displayed in Figure 8. The model produces layering artifacts in the expected parts of the records and with the expected signs and amplitudes. However, it is hard to reproduce the precise distribution of layering artifacts. This is due to the fact that the position of layering artifacts is random, and that the observed layering artifacts in an ice core record are one single outcome among many possibilities. The simple parametrization we derived thus appears to provide reasonable results for accumulation conditions ranging from 3.9 to $1.3\text{cm}\cdot\text{ie}\cdot\text{yr}^{-1}$, encompassing most of the climatic conditions of the East Antarctic plateau for both the glacial and interglacial periods.

3.3.3 Removing layered trapping artifacts

Since layered gas trapping artifacts are not due to chronologically ordered atmospheric variations, a proper interpretation of gas records requires them to be cleaned from the datasets. As pointed out by Fourteau et al. (2017), in some sections of the records these artifacts only exhibit negative or positive methane anomalies. They cannot therefore be removed by applying a running average without introducing bias in the signal.

To clean the new three methane signals presenting layering artifacts (EDC96, EDC99 and Vostok) we use the cleaning procedure described by Fourteau et al. (2017). Briefly, this cleaning algorithm starts by estimating a smooth signal that should

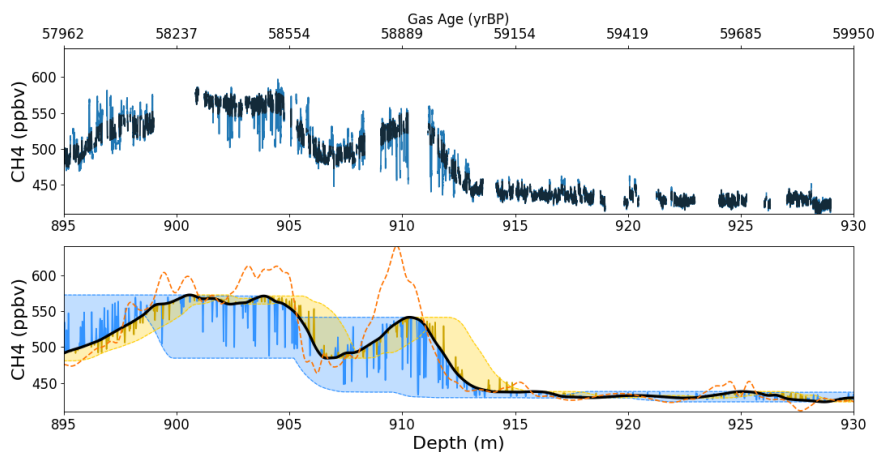


Figure 8. Same as Figure 2 for the DO17 Vostok section. The methane data of the upper panel are from Fourteau et al. (2017) and the atmospheric reference of the lower panel is from Rhodes et al. (2015).

represent the measured signal free of layering artifacts and analytical noise. For this purpose, a running median is first computed to remove the layering artifacts while minimizing bias. Then, the signal is smoothed with a binned average, and interpolated back to high resolution using an interpolating spline. Then, the analytical noise is estimated and the data clipped to remove artifacts larger than the analytical noise.

- 5 This procedure was successfully applied to the Holocene section of EDC99, that only exhibits a few artifacts. The resulting cleaned signal is displayed in the upper panel of Figure 4 as a black curve. However, direct application of this algorithm to the EDC96 DO6-9 and Vostok DO21 records leads to an ineffective removal of layering artifacts in periods of fast methane rise. After investigation, it appears that the main issue the algorithm is facing is the determination of an artifacts free signal by the rolling median. In some section of the ice cores, the signal displays high concentrations of artifacts with methane anomalies of
10 50ppbv or more, as seen for instance in the onset of the DO8 in Figure 5. In these conditions, the rolling median is influenced by the presence of the artifacts and yields a biased signal. To circumvent this problem, we manually provided a set of values that correspond to the artifact free part of the signal. As it is easy to distinguish the layering artifacts from the rest of the signal, the manual selection of these points is fairly unambiguous and straightforward. The rest of algorithm then proceeds as normal. The cleaned EDC99 Holocene, EDC96 DO6-9 and Vostok DO21 signals are displayed in the upper panels of Figures 5 and 6
15 in black.



3.4 Smoothing in East Antarctic ice cores

The five ice core sections measured in this article all originate from the East Antarctic plateau. The low temperatures and aridity of this region result in a slow densification of the firm, and a slow bubble closure. Therefore, the gas enclosed in a given ice layer tends to have a broad age distribution. This leads to an important smoothing of atmospheric fast variability observed in East Antarctic ice cores (Spahni et al., 2003; Joos and Spahni, 2008; Köhler et al., 2011; Ahn et al., 2014; Fourteau et al., 2017).

3.4.1 Estimating gas age distributions

Since smoothing in an ice core record is a direct consequence of the gas age distribution (GAD), the knowledge of GADs for various temperature and accumulation conditions is necessary to predict the impact of smoothing on gas signals. We thus apply the GAD extraction method proposed by Fourteau et al. (2017) to the five new high resolution records. This method, designed to estimate the GAD of low accumulation records, is based on the comparison with a weakly smoothed record from a high accumulation ice core, used as an atmospheric reference (see Section 3.2). An optimal log-normal age distribution is derived to best match the measured signal with the smoothing of the atmospheric reference by the GAD. Using a log-normal law allows to have a well-defined problem in the mathematical sense. A log-normal distribution is fully defined by two independent parameters. The GAD extraction problem is thus reduced to the recovery of a pair of optimal parameters. Nonetheless, log-normal laws exhibit a large range of shapes that can adequately represent the age distributions (Köhler et al., 2011; Fourteau et al., 2017). During the extraction procedure, a new gas age chronologies are produced for the low-accumulation records. They are constructed to be consistent with the already-existing chronologies of the high-accumulation atmospheric reference (Fourteau et al., 2017). The gas age distributions obtained for the five new ice core sections are displayed as solid lines in Figure 9, and an uncertainty analysis is available in Section S5 of the Supplement. The parameters defining the different log-normal distributions are listed in Table 1. The standard deviation in this table should not be directly interpreted as the broadness of the age distribution and therefore its degree of smoothing. Indeed, some distributions exhibit strong asymmetries that tend to increase the standard deviation values. For instance, the Vostok DO21 age distribution has a standard deviation value much larger than the other distributions, but does not induce a much larger smoothing.

3.4.2 Smoothing and accumulation

The degree of smoothing in a gas record is strongly linked to the accumulation rate under which the gases are trapped, with low accumulation sites exhibiting a stronger degree of smoothing (Spahni et al., 2003; Joos and Spahni, 2008; Köhler et al.,

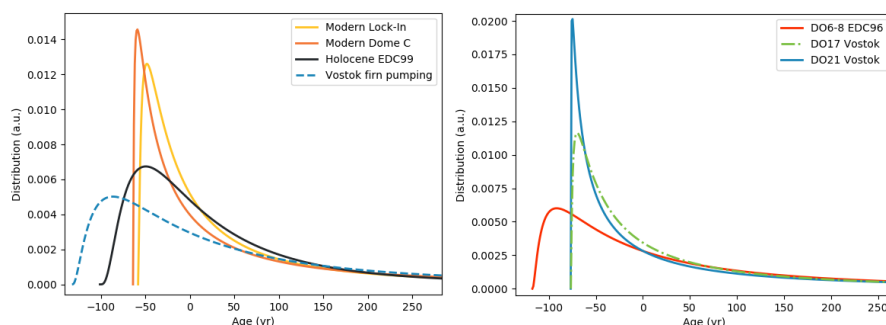


Figure 9. Gas age distributions in various ice cores. The distributions are centered around their median values. The left panel displays Holocene GADs and the right panel glacial period GADs. The DO21 Vostok, DO6-9 EDC96, Holocene EDC99 and modern Lock-In and Dome C age distributions shown as solid lines were determined in this study. The dashed Vostok DO17 distribution was also determined by comparison with a high-accumulation record (Fourteau et al., 2017). The dashed Vostok firn pumping distribution was obtained with a gas trapping model, constrained with firn air pumping data (Witrant et al., 2012).

Table 1. Parameters defining the log-normal gas age distributions derived by comparison with weakly smoothed records. The location and scale parameters correspond to the μ and σ parameters used to define the log-normal laws in Equation 1 of Köhler et al. (2011).

Site and Period	Location	Scale	Mean (yr)	Std Dev (yr)
Lock-In Modern	4.063	1.333	141	313
Dome C late Modern	4.156	1.611	234	823
Dome C 8.2ka	4.618	1.100	185	285
Dome C DO6-9	4.765	1.231	250	472
Vostok DO21	4.339	1.988	552	3950

2011). First, a lower accumulation is generally associated with a lower temperature. Low-temperature ice deforms less easily and the densification process is therefore slower and bubble closure spans a larger time period. Moreover, a low accumulation is also associated with a slow mechanical load increase of the ice material, also resulting in a slower densification and a longer bubble closure period.

5

Two new glacial period gas age distributions were derived in this work (EDC96 DO6-9 and Vostok DO21). This is to be added to the previously published GAD obtained for the Vostok site during the DO17 event using the same GAD extraction method ($1.3\text{cm}\cdot\text{ie}\cdot\text{yr}^{-1}$ accumulation rate; Fourteau et al., 2017). These three age distributions of East Antarctic sites under glacial conditions are displayed in the right panel of Figure 9. The smoothing they induce is represented for the DO6 to 9 and DO21 events in Figure 10. It appears that the two Vostok distributions lead to similar smoothing. On the other hand the GAD

10



obtained for EDC96 for the DO6-9 events is significantly broader than the Vostok ones and results in a stronger smoothing, especially visible on the onset of the DO21 event. This is surprising as the Vostok DO21 and Dome C DO6-9 records have the same accumulation rate, and should therefore present similar age distributions. However, the distributions obtained for glacial Vostok (DO17 and 21 events) also appear to be suited for the smoothing of DO6 to 9 events in EDC96, as seen in the lower panel of Figure 10. Moreover, the uncertainty analysis reveals that the distribution extracted from the EDC96 record is poorly constrained, with a large range of GADs resulting in adequate smoothing (Figure S11 in Section S5 of the supplement). It appears that the three glacial records exhibit similar degree of smoothing, and therefore enclose gases with the same gas age distribution. We propose to use a common gas age distribution to represent the smoothing in ice cores with accumulations below $2\text{cm}\cdot\text{ie}\cdot\text{yr}^{-1}$. The distribution proposed by Fourteau et al. (2017) is a good candidate for this common distribution, as it reproduces well the smoothing in the EDC96 DO6-9 record and the Vostok DO17 and 21 records. Moreover, its shape is a compromise between the two other glacial GADs proposed in this article (right panel of Figure 9). Finally, the similarity of the smoothing encountered during the DO17 and DO21 events suggests the absence of significant impurity effect on the GADs.

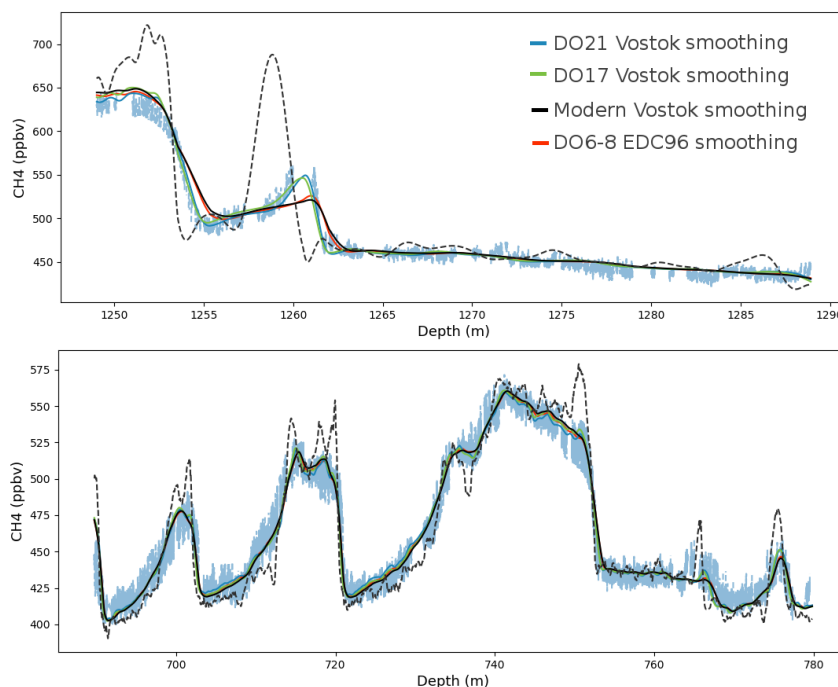


Figure 10. Comparison of smoothing for the three different glacial age distributions, and the modern Vostok GAD constrained with firn air pumping data. Atmospheric references (dashed lines) have been smoothed by the four different GADs and are displayed overlying the measurements (light blue). The upper panel shows the DO21 event as measured in Vostok, and the lower panel shows the DO-6 to 9 as measured in EDC96.



Comparing the typical GAD of the glacial period with the ones obtained for the Holocene and modern periods indicates that the later lead to a slightly smaller degree of smoothing. This illustrated with the smoothing of the 8.2ka event displayed in Figure 11. It is consistent with the expectation that the smoothing during the low-accumulation glacial period should be more important than during the higher-accumulation Holocene period. However, the doubling of accumulation between the DO17 event at Vostok and the 8.2ka event in EDC99 does not result in a drastic decrease of smoothing. It is also noteworthy that for the Dome C site, the transition from 8.2ka conditions ($3.1\text{cm}\cdot\text{ie}\cdot\text{yr}^{-1}$ accumulation rate) to modern conditions ($2.7\text{cm}\cdot\text{ie}\cdot\text{yr}^{-1}$ accumulation rate) does not significantly change the degree of smoothing. It thus appears that for accumulations below $3.9\text{cm}\cdot\text{ie}\cdot\text{yr}^{-1}$ the degree of smoothing only slowly increases with the diminution of the precipitation rate.

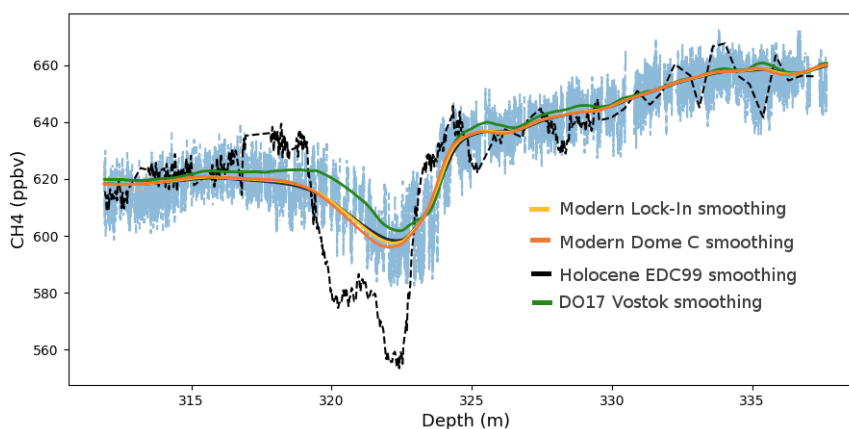


Figure 11. Comparison of the smoothing induced by three different Holocene and a modern age distributions. The atmospheric reference for the 8.2ka event (dashed line) has been smoothed by the four different GADs and displayed over the EDC99 measurements (light blue).

Finally, the expected smoothing using the firn pumping GAD estimation for modern Vostok is also displayed in Figure 10 in black (Witrant et al., 2012). This GAD was obtained with a method independent of the GAD extraction technique of this article. The smoothing estimated for modern Vostok is stronger than the one measured in the glacial Vostok ice core. This can be seen on the onset of the DO21, where the smoothing induced by the Vostok firn pumping distribution results in a signal with less variability than the CFA measurements. This confirms the observation of Fourteau et al. (2017) that the firn pumping GAD of modern Vostok leads to a stronger smoothing than the one observed during the DO17 event. This stronger smoothing in a modern ice core is in contradiction with the Holocene and modern GADs reported in this article for Dome C and Lock-In. This discrepancy could result from the large uncertainties associated with the firn-model-based GAD, which notably arise from the poor constraints on the closed porosity profiles used (Schaller et al., 2017). Unfortunately, high-resolution methane measurements of the late Holocene period in the Vostok ice core are not available to apply the GAD extraction method.



3.4.3 Effect of smoothing on record synchronization

Compared to the GADs of the Holocene and modern periods, the GADs of the glacial period exhibits a stronger degree of skewness (see Figure 9). This asymmetry of the distributions means that the smoothing not only removes variability, but also induces phase shifts during fast variations (Fourteau et al., 2017). This is especially visible on the variation recorded at depth
5 1260m in the Vostok DO21 ice core section, displayed in the upper panel of Figure 10. The peak of the event is recorded a couple of meters before its position in the absence of smoothing. In terms of ages, this corresponds to an error of about 85yr in the Vostok gas chronology. Studies relying on the synchronization of atmospheric variability between ice cores should be aware of this potential bias (Bazin et al., 2013; Veres et al., 2013). The best synchronization should either be performed on signals with a similar degree of smoothing, or the phase shifts should be taken into account in the age uncertainty estimates.

10 4 Loss of climatic information in a deep and thinned ice core from East Antarctica

East Antarctica is a region of particular interest for the drilling of deep ice cores. Indeed, thanks to low accumulation rates, it likely contains the oldest stratigraphically-undisturbed ice on earth. There is currently a search for very old ice, with ages potentially dating back one-and-a-half million years (Fischer et al., 2013; Passalacqua et al., 2018). When retrieved, such an ice core will be characterized by the gas trapping of low-accumulation East Antarctic plateau ice cores. Moreover, the old ice
15 will be located close to the bedrock and therefore will be thinned by strain.

In this section, we estimate the potential differences between atmospheric signals and their measurements in a theoretical one-and-a-half million years old ice core, for methane and carbon dioxide. For this purpose, we consider that the gas trapping occurs under an accumulation rate of $2\text{cm}\cdot\text{ie}\cdot\text{yr}^{-1}$. We suppose that the enclosed gases follow the age distribution obtained for Vostok during the DO17 period, established to be representative of East Antarctic glacial smoothing in Section 3.4.1. The
20 presence of layered trapping artifacts is simulated using the model parametrized in Section 3.3.2, with the assumption of high calcium variability. Finally, we assume that the thinning of the ice results in a resolution of $10,000\text{yr}\cdot\text{m}^{-1}$ (Passalacqua et al., 2018). This implies that a given ice layer at the bottom of the core is 200 times thinner than at the firm-ice transition. This has to be taken into account as analytical techniques have limited spatial resolutions below which variations are no longer resolved. In particular, layering artifacts will no longer be visible as individual events in the record.



4.1 Methane alterations

As a first case, we study the alterations of a methane record measured using a CFA system analogous to the one currently used at IGE. For the sake of simplicity, we assume that the atmospheric history recorded in this theoretical one-and-a-half million year-old ice core is similar to the DO15 to 17 events of the last glacial period. Hence, we simply use the WD CFA methane measurements as the atmospheric reference (Rhodes et al., 2015). We first determine the initially enclosed signal using the layering artifacts and smoothing models, and apply a 200 times thinning factor. The resulting signal is displayed in blue in the upper panel of Figure 12. Then, we simulate the process of CH₄ measurements by applying the smoothing induced by the CFA system. For this, we use the CFA impulse response derived by Fourteau et al. (2017). The end result is displayed in blue in the lower panel of Figure 12. The layering artifacts are no longer visible as they have been smoothed out by the CFA measurement. However, they affect the measured signal due to their asymmetry. This is illustrated by the difference between the blue and green curves in the lower panel of Figure 12, that respectively represent the CFA measurements with and without the presence of layering artifacts. However, even during periods of strong methane variations, the bias specifically due to layering artifacts does not exceed 10ppbv. This is of the order of the analytical noise usually observed with the CFA system (Fourteau et al., 2017). It therefore appears that layering artifacts only negligibly affect the measured signal in the case of thinned ice cores. However, the potential impact of layering artifacts is sensitive to the parameters of the layering model. Notably, increasing the number of anomalous layers increases the amplitude of the biases.

The internal smoothing of the CFA system also tends to deteriorate information recorded in the ice core by attenuating fast variability. It is therefore important to determine to what extent CFA smoothing adds to the already present firm smoothing. To study this point, we compare the frequency responses of the CFA system and firm smoothing. These frequency responses represent the attenuation experienced by a sine signal, as a function of the sine period. To achieve this, we first expressed the CFA impulse response (its smoothing function) on a gas age scale, taking into account the thinning of the ice. Then, the frequency responses were deduced using fast Fourier transforms. The gas age distribution and the CFA impulse response are displayed in the left panel of Figure 13 with the frequency responses in the right panel. For sine periods longer than 100yr the firm smoothing is larger than the CFA smoothing. Yet, for a sine period of 500yr the firm induces a smoothing of 50% while the CFA system smooths by about 20%. The CFA smoothing is therefore noticeable and adds to the already present firm smoothing. This is illustrated in the lower panel of Figure 12, where the difference between the black and green curves is due to the presence of CFA smoothing. The influence of this analytical smoothing would be even stronger in the case of a narrower gas age distribution, for instance during interglacial periods. This is problematic as it deteriorates climatic information still

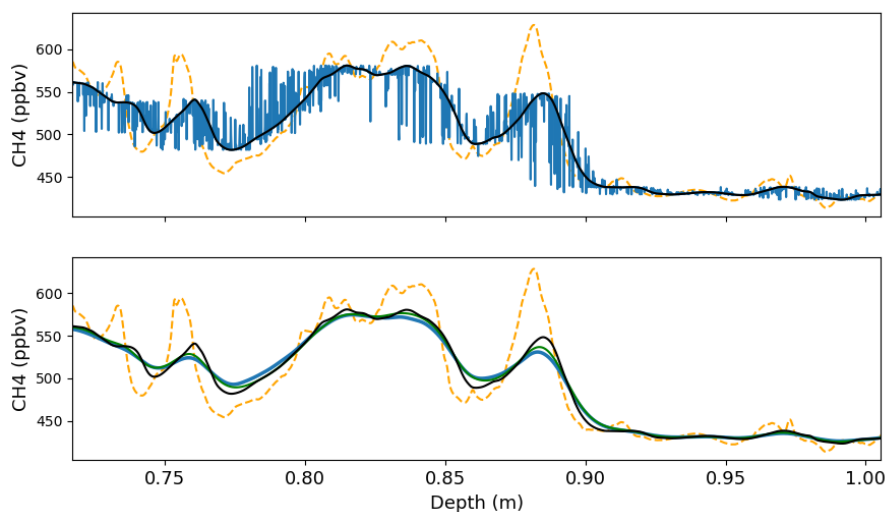


Figure 12. Impacts of layered trapping and smoothing on a synthetic million-and-a-half years old methane record. Upper panel: signal recorded in the ice taking into account smoothing (in black) and layered trapping artifacts (in blue). The atmospheric reference is displayed in orange. The depth scale takes into account the thinning of the ice. Lower panel: CFA measurements with (in blue) and without layering artifacts (in green). The atmospheric reference is displayed orange and the initial recorded signal without layering artifacts is also displayed in black.

present in the gas record. It thus appears important to improve current CFA gas systems in order to minimize their internal smoothing, in order to take full advantage of the gas records entrapped in deep ice cores.

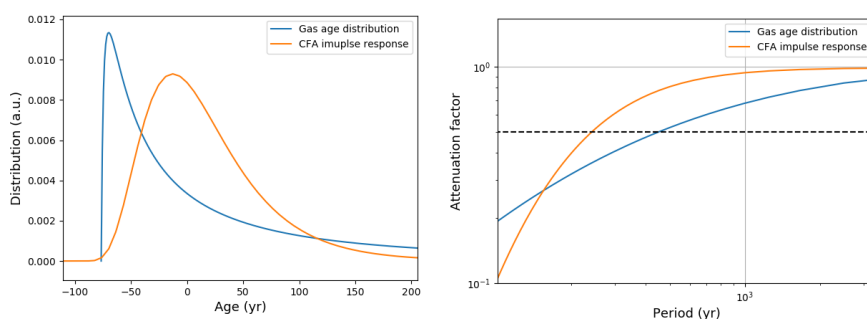


Figure 13. Left panel: gas age distribution in the synthetic million-and-a-half years old ice core in blue, and CFA impulse response on a gas age scale in orange. Right panel: attenuation of a sine signal by the firm and CFA smoothing in blue and orange respectively. The horizontal dashed line indicates the 50% attenuation.



4.2 Carbon dioxide alterations

So far in this article only methane records have been considered. However, smoothing and layering artifacts also potentially affect other gaseous records, such as carbon dioxide records. Since CO₂ is one of the principal and most studied greenhouse gases, we propose to quantify the potential impacts of gas trapping on the record enclosed in a million-and-a-half years old ice core. Similar to the methane case of the previous section, we used the CO₂ measurements of the high accumulation WD ice core as the atmospheric reference (Marcott et al., 2014). The chosen data points correspond to the last deglaciation, as they constitute a fast atmospheric increase of CO₂. As for CH₄, the synthetic ice core signal is determined with the smoothing and layering model and ice layers are thinned 200 times. Finally, we emulate the process of discrete measurements. For that, we assume that the final ice core is continuously discretized into 4cm thick pieces, and that the measured value is the average value of the concentrations enclosed in the ice piece.

The results are displayed in Figure 14. The ice core signal is displayed in blue in the left panel of Figure 14, with the artifact free record superimposed in black. It can be seen that during enclosure, the layering heterogeneities can produce artifacts reaching up to 10ppmv. The measurements obtained by a discrete method are displayed on the right side of Figure 14 with and without the presence of layering artifacts in blue and black respectively. These results show that the impact of layering artifacts on the final measurements does not exceed 0.5ppmv, even during abrupt CO₂ rises. However, as for methane the impact of the layering artifacts is sensitive to the amount of abnormal layers per meter.

We also compared the rate of change of carbon dioxide in the atmospheric reference and in the measured record. For some of the fast variations of atmospheric CO₂, a reduced rate of change is deduced from the ice core record. A specific example (the deeper part of the records in Figure 14) is shown in Figure 15, where the rates of change of CO₂ in the atmosphere, recorded in the ice, and deduced from discrete measurements are compared. For this event, the atmospheric rate of change peaks at about 0.055ppmv.yr⁻¹, while the corresponding imprint in the ice has only a rate of change of 0.035ppmv.yr⁻¹ due to firn smoothing. The process of discrete measurement further diminishes the measured rate of change to about 0.02ppmv.yr⁻¹, a bit more than a third of the atmospheric value.

5 Conclusions

This work evaluated two gas trapping effects that affect the recorded atmospheric trace gas history in polar ice cores. The first one is the layered gas trapping, that produces stratigraphic heterogeneities appearing as spurious values in the measured record (Rhodes et al., 2016). The second one is the smoothing effect that removes a part of the variability in the gas records (Spahni

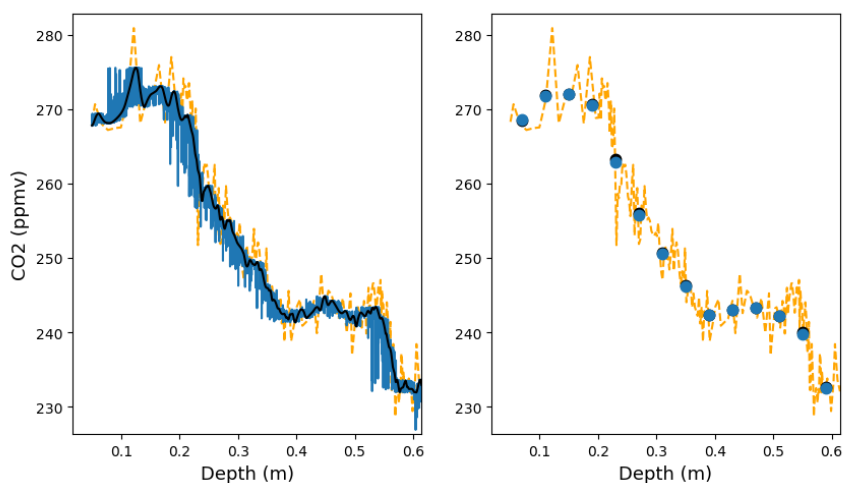


Figure 14. Impacts of layered trapping and smoothing on a synthetic million-and-a-half years old carbon dioxide record. Left panel: recorded signal in the ice taking into account smoothing (in black) and layered trapping artifacts (in blue). The atmospheric reference is shown in orange. Right panel: measured signal by a discrete system shown as blue points. The atmospheric reference (in orange) and the measured signal without layering artifacts (black points) are also displayed.

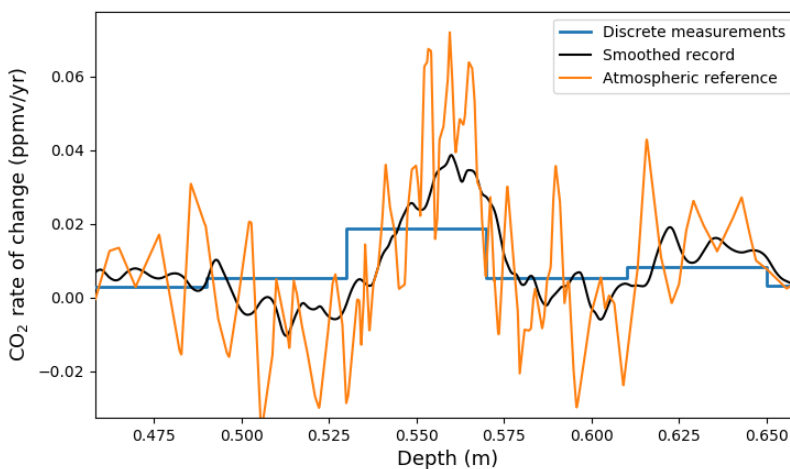


Figure 15. Impact of gas trapping processes and measurements on the CO₂ rate of change. The rate of change of the atmosphere is displayed in orange, while the rate change recorded in the ice is in black, and the measured one is in blue.

et al., 2003; Joos and Spahni, 2008; Köhler et al., 2011). Our work focuses on the arid region of East Antarctica, as this is where the oldest ice cores are retrieved. Five new sections from East Antarctic ice cores have been analyzed at high resolution for methane concentration.



The characterization of layering artifacts in these new measurements is consistent with the physical mechanisms already proposed in the literature (Etheridge et al., 1992; Rhodes et al., 2016). In accordance with previous studies (Hörhold et al., 2012; Fujita et al., 2016), the data suggest that chemistry could promote the presence of especially dense layers closing in advance and creating the layering artifacts. We parameterized a simple model to reproduce the observed distribution and characteristics
5 of layering artifacts, and were able to find a common set of parameters to reproduce the measured artifacts in all studied East Antarctic ice cores.

In order to constrain the smoothing effect, we estimated the gas age distributions in each of the five ice core sections. For this purpose, we use the method proposed by Fourteau et al. (2017) based on the comparison with higher accumulation methane records. It appears that during the last glacial period, the different methane records in ice cores formed under accumulation rates
10 lower than 2cm.ice.yr^{-1} all display similar degree of smoothing. We therefore propose to use a common gas age distribution for glacial East Antarctic sites with accumulations below 2cm.ice.yr^{-1} . The comparison of the glacial and interglacial GADs suggests that the smoothing is higher at Dome C during the glacial period than during the interglacial period. Yet, despite a doubling of accumulation during the interglacial period, the resulting smoothing is only slightly lower. Similarly to Fourteau et al. (2017), we observed that the smoothing during the glacial in the Vostok ice core is weaker than the one predicted for
15 modern Vostok by the age distribution estimated by gas trapping models (Witrant et al., 2012).

Finally, we applied our methodology to the theoretical case of a million-and-a-half years old ice core drilled on the East Antarctic plateau. Our results suggest that due to thinning, the layering artifacts will no longer be resolved during measurements. However, it appears that their potential influence on the end result measurements is rather low, with impacts below
20 10ppbv and 0.5ppmv for methane and carbon dioxide respectively. In the case of methane variations during DO events, most of the record alterations originate from the firn smoothing. Yet, the limited spatial resolution of the CFA system induces a smoothing that is not entirely negligible compared to the one of the firn. For carbon dioxide, firn smoothing appears to significantly diminish the recorded rates of change of abrupt CO_2 increases, compared to their atmospheric values. The estimations of CO_2 rates of change are further altered by the process of discrete measurement, and measured values can be three time lower than the actual atmospheric rate of change.

25 *Code availability.* The programs used for data processing and modeling were developed using python3 and available packages. They will be provided upon request to the corresponding authors.



Data availability. The high resolution methane datasets will be made available on the World Data Center for Paleoclimatology.

Author contributions. This scientific project was designed by JC, XF, KF, and PM. JC and PM participated in the Lock-In drilling and XF participated in the shallow Dome C drilling. AAE and VL made available and pre-processed the Vostok ice core section. The high resolution methane measurements were carried out by XF and KF. The codes for data processing and modeling were developed by KF and PM. All
5 authors contributed to the interpretation of the data. The manuscript was written by KF with the help of all co-authors.

Competing interests. The authors declare having no competing interests

Disclaimer. TEXT

Acknowledgements. This work is a contribution to EPICA, a joint European Science Foundation/European Commission scientific program funded by the European Union and national contributions from Belgium, Denmark, France, Germany, Italy, the Netherlands, Norway, Swe-
10 den, Switzerland, and the United Kingdom. The Vostok ice core was made accessible in the framework of the Laboratoire International Associé (LIA) Vostok. The Lock-In drilling was supported by the IPEV project No 1153 and the European Community's Seventh Frame-
work Programme under grant agreement No291062 (ERC ICE&LASERS). We are grateful to the Lock-In field personnel: David Colin, Phillippe Dordhain, and Phillippe Possenti who performed the drilling, as well as Patrice Godon for setting up the logistics. The shallow Dome
15 C drilling was performed by Phillippe Possenti and supported by the IPEV project No 902 and the French ANR program RPD COCLICO
(ANR-10-RPDO-002-01). We thank Robert Mulvaney and the British Antarctic Survey for the Fletcher promontory ice core drilling, and the permission to use the Fletcher methane data. We thank Grégoire Aufresne for his help processing the ice cores. We thank Grégory Teste for his help during the ice core processing and the CFA methane measurements. We thank Jochen Schmitt and Hubertus Fischer for their constructive comments. This work was supported by the French INSU/CNRS LEFE projects NEVE-CLIMAT and HEPIGANE. This work was also supported by the French ANR programs RPD COCLICO (ANR-10-RPDO-002-01). This is EPICA publication no. XX.



References

- Ahn, J., Brook, E. J., and Buizert, C.: Response of atmospheric CO₂ to the abrupt cooling event 8200 years ago, *Geophys. Res. Lett.*, 41, 604–609, <https://doi.org/10.1002/2013gl058177>, 2014.
- Arnaud, L., Barnola, J.-M., and Duval, P.: Physical modeling of the densification of snow/firn and ice in the upper part of polar ice sheets, *Phys. Ice Core Rec.*, pp. 285–305, <http://hdl.handle.net/2115/32472>, 2000.
- Bazin, L., Landais, A., Lemieux-Dudon, B., Toyé Mahamadou Kele, H., Veres, D., Parrenin, F., Martinerie, P., Ritz, C., Capron, E., Lipenkov, V. Y., Loutre, M.-F., Raynaud, D., Vinther, B., Svensson, A., Rasmussen, S. O., Severi, M., Blunier, T., Leuenberger, M., Fischer, H., Masson-Delmotte, V., Chappellaz, J., and Wolff, E. W.: An optimized multi-proxy, multi-site Antarctic ice and gas orbital chronology (AICC2012): 120-800 ka, *Clim. Past*, 9, 1715–1731, <https://doi.org/10.5194/cp-9-1715-2013>, 2013.
- 10 Bock, J., Martinerie, P., Witrant, E., and Chappellaz, J.: Atmospheric impacts and ice core imprints of a methane pulse from clathrates, *Earth Planet. Sci. Lett.*, 349-350, 98 – 108, <https://doi.org/https://doi.org/10.1016/j.epsl.2012.06.052>, 2012.
- Bréant, C., Martinerie, P., Orsi, A., Arnaud, L., and Landais, A.: Modelling firn thickness evolution during the last deglaciation: constraints on sensitivity to temperature and impurities, *Clim. Past*, 13, 833–853, <https://doi.org/10.5194/cp-13-833-2017>, 2017.
- Buizert, C., Martinerie, P., Petrenko, V. V., Severinghaus, J. P., Trudinger, C. M., Witrant, E., Rosen, J. L., Orsi, A. J., Rubino, M.,
15 Etheridge, D. M., Steele, L. P., Hogan, C., Laube, J. C., Sturges, W. T., Levchenko, V. A., Smith, A. M., Levin, I., Conway, T. J., Dlugokencky, E. J., Lang, P. M., Kawamura, K., Jenk, T. M., White, J. W. C., Sowers, T., Schwander, J., and Blunier, T.: Gas transport in firn: multiple-tracer characterisation and model intercomparison for NEEM, Northern Greenland, *Atmos. Chem. Phys.*, 12, 4259–4277, <https://doi.org/10.5194/acp-12-4259-2012>, 2012.
- Buizert, C., Cuffey, K. M., Severinghaus, J. P., Baggenstos, D., Fudge, T. J., Steig, E. J., Markle, B. R., Winstrup, M., Rhodes, R. H., Brook,
20 E. J., Sowers, T. A., Clow, G. D., Cheng, H., Edwards, R. L., Sigl, M., McConnell, J. R., and Taylor, K. C.: The WAIS Divide deep ice core WD2014 chronology-Part 1: methane synchronization (68-31 ka BP) and the gas age-ice age difference, *Clim. Past*, 11, 153–173, <https://doi.org/10.5194/cp-11-153-2015>, 2015.
- Chappellaz, J., Stowasser, C., Blunier, T., Baslev-Clausen, D., Brook, E. J., Dallmayr, R., Faïn, X., Lee, J. E., Mitchell, L. E., Pascual, O., Romanini, D., Rosen, J., and Schüpbach, S.: High-resolution glacial and deglacial record of atmospheric methane by continuous-flow and
25 laser spectrometer analysis along the NEEM ice core, *Clim. Past*, 9, 2579–2593, <https://doi.org/10.5194/cp-9-2579-2013>, 2013.
- Dällenbach, A., Blunier, T., Flückiger, J., Stauffer, B., Chappellaz, J., and Raynaud, D.: Changes in the atmospheric CH₄ gradient between Greenland and Antarctica during the Last Glacial and the transition to the Holocene, *Geophys. Res. Lett.*, 27, 1005–1008, <https://doi.org/10.1029/1999GL010873>, 2000.
- Etheridge, D. M., Pearman, G. I., and Fraser, P. J.: Changes in tropospheric methane between 1841 and 1978 from a high accumulation-rate
30 Antarctic ice core, *Tellus B Chem. Phys. Meteorol.*, 44, 282–294, <https://doi.org/10.3402/tellusb.v44i4.15456>, 1992.



- Fischer, H., Severinghaus, J., Brook, E., Wolff, E. W., Albert, M., Alemany, O., Arthern, R., Bentley, C., Blankenship, D., Chappellaz, J., Creyts, T., Dahl-Jensen, D., Dinn, M., Frezzotti, M., Fujita, S., Gallee, H., Hindmarsh, R., Hudspeth, D., Jugie, G., Kawamura, K., Lipenkov, V. Y., Miller, H., Mulvaney, R., Parrenin, F., Pattyn, F., Ritz, C., Schwander, J., Steinhage, D., van Ommen, T., and Wilhelms, F.: Where to find 1.5 million yr old ice for the IPICS "Oldest-Ice" ice core, *Clim. Past*, 9, 2489–2505, <https://doi.org/10.5194/cp-9-2489-2013>, 2013.
- 5
- Fourteau, K., Faïn, X., Martinerie, P., Landais, A., Ekaykin, A. A., Lipenkov, V. Y., and Chappellaz, J.: Analytical constraints on layered gas trapping and smoothing of atmospheric variability in ice under low-accumulation conditions, *Clim. Past*, 13, 1815–1830, <https://doi.org/10.5194/cp-13-1815-2017>, 2017.
- Fourteau, K., Martinerie, P., Faïn, X., Schaller, C. F., Tuckwell, R. J., Löwe, H., Arnaud, L., Magand, O., Thomas, E. R., Freitag, J., Mulvaney, R., Schneebeli, M., and Lipenkov, V. Y.: Multi-tracer study of gas trapping in an East Antarctic ice core, *Cryosphere Discuss.*, 2019, 1–34, <https://doi.org/10.5194/tc-2019-89>, 2019.
- 10
- Freitag, J., Wilhelms, F., and Kipfstuhl, S.: Microstructure-dependent densification of polar firn derived from X-ray microtomography, *J. Glaciol.*, 50, 243–250, <https://doi.org/10.3189/172756504781830123>, 2004.
- Freitag, J., Kipfstuhl, S., Laepple, T., and Wilhelms, F.: Impurity-controlled densification: a new model for stratified polar firn, *J. Glaciol.*, 59, 1163–1169, <https://doi.org/10.3189/2013Jog13J042>, 2013.
- 15
- Fujita, S., Okuyama, J., Hori, A., and Hondoh, T.: Metamorphism of stratified firn at Dome Fuji, Antarctica: A mechanism for local insolation modulation of gas transport conditions during bubble close off, *J. Geophys. Res. Earth Surf.*, 114, F03023, <https://doi.org/10.1029/2008JF001143>, 2009.
- Fujita, S., Goto-Azuma, K., Hirabayashi, M., Hori, A., Iizuka, Y., Motizuki, Y., Motoyama, H., and Takahashi, K.: Densification of layered firn in the ice sheet at Dome Fuji, Antarctica, *J. Glaciol.*, 62, 103–123, <https://doi.org/10.1017/jog.2016.16>, 2016.
- 20
- Gautier, E., Savarino, J., Erbland, J., Lanciki, A., and Possenti, P.: Variability of sulfate signal in ice core records based on five replicate cores, *Clim. Past*, 12, 103–113, <https://doi.org/10.5194/cp-12-103-2016>, 2016.
- Gregory, S. A., Albert, M. R., and Baker, I.: Impact of physical properties and accumulation rate on pore close-off in layered firn, *Cryosphere*, 8, 91–105, <https://doi.org/10.5194/tc-8-91-2014>, 2014.
- 25
- Hörhold, M. W., Kipfstuhl, S., Wilhelms, F., Freitag, J., and Frenzel, A.: The densification of layered polar firn, *J. Geophys. Res. Earth Surf.*, 116, <https://doi.org/10.1029/2009jf001630>, 2011.
- Hörhold, M. W., Laepple, T., Freitag, J., Bigler, M., Fischer, H., and Kipfstuhl, S.: On the impact of impurities on the densification of polar firn, *Earth Planet. Sci. Lett.*, 325, 93–99, <https://doi.org/10.1016/j.epsl.2011.12.022>, 2012.
- Huber, C., Leuenberger, M., Spahni, R., Flückiger, J., Schwander, J., Stocker, T. F., Johnsen, S., Landais, A., and Jouzel, J.: Isotope calibrated Greenland temperature record over Marine Isotope Stage 3 and its relation to CH₄, *Earth Planet. Sci. Lett.*, 243, 504–519, 2006.
- 30
- Joos, F. and Spahni, R.: Rates of change in natural and anthropogenic radiative forcing over the past 20,000 years, *Proc. Natl. Acad. Sci. USA*, 105, 1425–1430, <https://doi.org/10.1073/pnas.0707386105>, 2008.



- Köhler, P., Knorr, G., Buiron, D., Lourantou, A., and Chappellaz, J.: Abrupt rise in atmospheric CO₂ at the onset of the Bølling/Allerød: in-situ ice core data versus true atmospheric signal, *Clim. Past*, 7, 473–486, <https://doi.org/10.5194/cp-7-473-2011>, 2011.
- Lambert, F., Bigler, M., Steffensen, J. P., Hutterli, M., and Fischer, H.: Centennial mineral dust variability in high-resolution ice core data from Dome C, Antarctica, *Clim. Past*, 8, 609–623, <https://doi.org/10.5194/cp-8-609-2012>, 2012.
- 5 Loulergue, L., Schilt, A., Spahni, R., Masson-Delmotte, V., Blunier, T., Lemieux, B., Barnola, J.-M., Raynaud, D., Stocker, T. F., and Chappellaz, J.: Orbital and millennial-scale features of atmospheric CH₄ over the past 800,000 years, *Nature*, 453, 383–386, <https://doi.org/10.1038/nature06950>, 2008.
- Lüthi, D., Floch, M. L., Bereiter, B., Blunier, T., Barnola, J.-M., Siegenthaler, U., Raynaud, D., Jouzel, J., Fischer, H., Kawamura, K., and Stocker, T. F.: High-resolution carbon dioxide concentration record 650,000– 800,000 years before present, *Nature*, 453, 379–382,
10 <https://doi.org/10.1038/nature06949>, 2008.
- Marcott, S. A., Bauska, T. K., Buizert, C., Steig, E. J., Rosen, J. L., Cuffey, K. M., Fudge, T. J., Severinghaus, J. P., Ahn, J., Kalk, M. L., McConnell, J. R., Sowers, T., Taylor, K. C., White, J. W. C., and Brook, E. J.: Centennial-scale changes in the global carbon cycle during the last deglaciation, *Nature*, 514, 616–619, <https://doi.org/10.1038/nature13799>, 2014.
- Martín, C. and Gudmundsson, G. H.: Effects of nonlinear rheology, temperature and anisotropy on the relationship between age and depth at
15 ice divides, *Cryosphere*, 6, 1221–1229, <https://doi.org/10.5194/tc-6-1221-2012>, 2012.
- Martinerie, P., Raynaud, D., Etheridge, D. M., Barnola, J.-M., and Mazaudier, D.: Physical and climatic parameters which influence the air content in polar ice, *Earth Planet. Sc. Lett.*, 112, 1–13, [https://doi.org/10.1016/0012-821x\(92\)90002-d](https://doi.org/10.1016/0012-821x(92)90002-d), 1992.
- Mitchell, L., Brook, E., Lee, J. E., Buizert, C., and Sowers, T.: Constraints on the Late Holocene Anthropogenic Contribution to the Atmospheric Methane Budget, *Science*, 342, 964–966, <https://doi.org/10.1126/science.1238920>, 2013.
- 20 Mitchell, L. E., Buizert, C., Brook, E. J., Breton, D. J., Fegyveresi, J., Baggenstos, D., Orsi, A., Severinghaus, J., Alley, R. B., Albert, M., Rhodes, R. H., McConnell, J. R., Sigl, M., Maselli, O., Gregory, S., and Ahn, J.: Observing and modeling the influence of layering on bubble trapping in polar firn, *J. Geophys. Res. Atmos.*, 120, 2558–2574, <https://doi.org/10.1002/2014jd022766>, 2015.
- Morville, J., Kassi, S., Chenevier, M., and Romanini, D.: Fast, low-noise, mode-by-mode, cavity-enhanced absorption spectroscopy by diode-laser self-locking, *Appl. Phys. B-Lasers O.*, 80, 1027–1038, <https://doi.org/10.1007/s00340-005-1828-z>, 2005.
- 25 Parrenin, F., Petit, J.-R., Masson-Delmotte, V., Wolff, E., Basile-Doelsch, I., Jouzel, J., Lipenkov, V., Rasmussen, S. O., Schwander, J., Severi, M., Udisti, R., Veres, D., and Vinther, B. M.: Volcanic synchronisation between the EPICA Dome C and Vostok ice cores (Antarctica) 0–145 kyr BP, *Clim. Past*, 8, 1031–1045, <https://doi.org/10.5194/cp-8-1031-2012>, 2012.
- Passalacqua, O., Cavitte, M., Gagliardini, O., Gillet-Chaulet, F., Parrenin, F., Ritz, C., and Young, D.: Brief communication: Candidate sites of 1.5 Myr old ice 37 km southwest of the Dome C summit, East Antarctica, *Cryosphere*, 12, 2167–2174, <https://doi.org/10.5194/tc-12-2167-2018>, 2018,
30
- Raymond, C. F.: Deformation in the Vicinity of Ice Divides, *J. Glaciol.*, 29, 357–373, <https://doi.org/10.3189/S0022143000030288>, 1983.



- Rhodes, R. H., Faïn, X., Stowasser, C., Blunier, T., Chappellaz, J., McConnell, J. R., Romanini, D., Mitchell, L. E., and Brook, E. J.: Continuous methane measurements from a late Holocene Greenland ice core: atmospheric and in-situ signals, *Earth Planet. Sc. Lett.*, 368, 9–19, <https://doi.org/10.1016/j.epsl.2013.02.034>, 2013.
- Rhodes, R. H., Brook, E. J., Chiang, J. C. H., Blunier, T., Maselli, O. J., McConnell, J. R., Romanini, D., and Severinghaus, J. P.: Enhanced tropical methane production in response to iceberg discharge in the North Atlantic, *Science*, 348, 1016–1019, <https://doi.org/10.1126/science.1262005>, 2015.
- Rhodes, R. H., Faïn, X., Brook, E. J., McConnell, J. R., Maselli, O. J., Sigl, M., Edwards, J., Buizert, C., Blunier, T., Chappellaz, J., and Freitag, J.: Local artifacts in ice core methane records caused by layered bubble trapping and in situ production: a multi-site investigation, *Clim. Past*, 12, 1061–1077, <https://doi.org/10.5194/cp-12-1061-2016>, 2016.
- 10 Rommelaere, V., Arnaud, L., and Barnola, J.-M.: Reconstructing recent atmospheric trace gas concentrations from polar firn and bubbly ice data by inverse methods, *J. Geophys. Res. Atmos.*, 102, 30 069–30 083, <https://doi.org/10.1029/97jd02653>, 1997.
- Salamatin, A. N., Lipenkov, V. Y., Barnola, J. M., Hori, A., Duval, P., and Hondoh, T.: Snow/firn densification in polar ice sheets, *Low Temperature Science*, 68, 195–222, 2009.
- Schaller, C. F., Freitag, J., and Eisen, O.: Critical porosity of gas enclosure in polar firn independent of climate, *Clim. Past*, 13, 1685–1693, <https://doi.org/10.5194/cp-13-1685-2017>, 2017.
- Schwander, J.: The transformation of snow to ice and the occlusion of gases, in: *The environmental record in glaciers and ice sheets*, edited by Oeschger, H. and Langway, C. C. J., pp. 53–67, John Wiley, New York, 1989.
- Schwander, J., Stauffer, B., and Sigg, A.: Air mixing in firn and the age of the air at pore close-off, *Ann. Glaciol.*, 10, 141–145, <https://doi.org/10.1017/S0260305500004328>, 1988.
- 20 Schwander, J., Barnola, J.-M., Andrié, C., Leuenberger, M., Ludin, A., Raynaud, D., and Stauffer, B.: The age of the air in the firn and the ice at Summit, Greenland, *J. Geophys. Res. Atmos.*, 98, 2831–2838, <https://doi.org/10.1029/92jd02383>, 1993.
- Shakun, J. D., Clark, P. U., He, F., Marcott, S. A., Mix, A. C., Liu, Z., Otto-Bliesner, B., Schmittner, A., and Bard, E.: Global warming preceded by increasing carbon dioxide concentrations during the last deglaciation, *Nature*, 484, 49–54, <https://doi.org/10.1038/nature10915>, 2012.
- 25 Spahni, R., Schwander, J., Flückiger, J., Stauffer, B., Chappellaz, J., and Raynaud, D.: The attenuation of fast atmospheric CH₄ variations recorded in polar ice cores, *Geophys. Res. Lett.*, 30, <https://doi.org/10.1029/2003gl017093>, 2003.
- Stauffer, B., Schwander, J., and Oeschger, H.: Enclosure of air during metamorphosis of dry firn to ice, *Ann. Glaciol.*, 6, 108–112, <https://doi.org/10.3189/1985AoG6-1-108-112>, 1985.
- Thomas, E. R., Wolff, E. W., Mulvaney, R., Steffensen, J. P., Johnsen, S. J., Arrowsmith, C., White, J. W., Vaughn, B., and Popp, T.: The 8.2 ka event from Greenland ice cores, *Quat. Sci. Rev.*, 26, 70–81, <https://doi.org/10.1016/j.quascirev.2006.07.017>, 2007.
- 30 Van Liefferinge, B. and Pattyn, F.: Using ice-flow models to evaluate potential sites of million year-old ice in Antarctica, *Clim. Past*, 9, 2335–2345, <https://doi.org/10.5194/cp-9-2335-2013>, 2013.



- Veres, D., Bazin, L., Landais, A., Toyé Mahamadou Kele, H., Lemieux-Dudon, B., Parrenin, F., Martinerie, P., Blayo, E., Blunier, T., Capron, E., Chappellaz, J., Rasmussen, S. O., Severi, M., Svensson, A., Vinther, B., and Wolff, E. W.: The Antarctic ice core chronology (AICC2012): an optimized multi-parameter and multi-site dating approach for the last 120 thousand years, *Clim. Past*, 9, 1733–1748, <https://doi.org/10.5194/cp-9-1733-2013>, 2013.
- 5 Witrant, E. and Martinerie, P.: Input Estimation from Sparse Measurements in LPV Systems and Isotopic Ratios in Polar Firns, *IFAC Proc. Vol.*, 46, 659 – 664, <https://doi.org/10.3182/20130204-3-FR-2033.00201>, 5th IFAC Symposium on System Structure and Control, 2013.
- Witrant, E., Martinerie, P., Hogan, C., Laube, J. C., Kawamura, K., Capron, E., Montzka, S. A., Dlugokencky, E. J., Etheridge, D., Blunier, T., and Sturges, W. T.: A new multi-gas constrained model of trace gas non-homogeneous transport in firn: evaluation and behaviour at eleven polar sites, *Atmos. Chem. Phys.*, 12, 11 465–11 483, <https://doi.org/10.5194/acp-12-11465-2012>, 2012.
- 10 Yeung, L. Y., Murray, L. T., Martinerie, P., Witrant, E., Hu, H., Banerjee, A., Orsi, A., and Chappellaz, J.: Isotopic constraint on the twentieth-century increase in tropospheric ozone, *Nature*, 570, 224–227, <https://doi.org/10.1038/s41586-019-1277-1>, 2019.